DESIGN OF THE ULTRAWIDEBAND ANTENNA WITH A QUADRUPLE-BAND REJECTION CHARACTERISTICS USING A COMBINATION OF THE COMPLEMENTARY SPLIT RING RESONATORS

D.-O. Kim, N.-I Jo, H.-A. Jang, and C.-Y. Kim

School of the Electronics Engineering
Kyungpook National University
Sankyuk-dong Puk-gu, Daegu 702-701, South Korea

Abstract—In this paper, the design method of a quadruple-band rejection ultra-wideband (UWB) antenna with three co-directional complementary split ring resonators (CSRRs) is proposed. Within the design step, individual antennas corresponding to each rejection band is first designed, and then a finalized structure is determined by assembling these individual antennas altogether. The shape of the final antenna achieves both the impedance matching of ultra-wideband and the respective resonances at four rejection bands. Here, the mutual coupling among the band rejection elements is minimized, and the placement of the resonators is optimized. The fabricated antenna is compact enough to be integrated into the UWB system, and also the measured results show the validity of the proposed design strategy.

1. INTRODUCTION

With the rapid development of wireless communication, the radio environment of the UWB system has coexisted with other narrow band communication systems. Namely the UWB antennas have encountered a hostile radio environment which has a great potential for radio interference by other systems that have the UWB bands (3.1–10.6 GHz) or have neighboring RF system bands. For instance, Wireless Local Area Network (WLAN) bands are 2.4 GHz (2.4–2.484 GHz), 5.2 GHz (5.15–5.35 GHz), and 5.8 GHz (5.725–5.825 GHz). World Interoperability for Microwave Access (WiMAX) system bands are

2.5 GHz (2.5–2.69 GHz), 3.5 GHz (3.4–3.69 GHz), and 5.8 GHz (5.25–5.825 GHz). In addition to these data communication system bands, some satellite service bands are the International Telecommunication Union (ITU) 8 GHz band and the Satellite Digital Multimedia Broadcasting (S-DMB) band 2.63–2.655 GHz [1]. Hence, the UWB RF front-ends may require an inclusion of many band-rejection filters to avoid possible interference from other communication systems. This may give rise to complications, an increase in size and cost, as well as an insertion-loss problem for the UWB systems. To solve these problems, this paper offers a new design process of adding a multi-band rejection function to the UWB antenna.

Many design techniques of band rejection performance being added to UWB antennas have already been proposed. The common and simple method is to insert the band rejection elements on the radiation patch of the UWB antenna. This would include various shape slots or parasitic elements [2–8]. The multi-band rejection UWB antennas have also been recently reported on some authors [9–18]. However, all of these antennas have two limitations in their design when it comes to adding a number of band rejection elements. One is a problem of the mutual coupling among the given elements, and the other trouble is the space restriction in the substrate of the compact UWB antenna. Due to these limitations, the quadruple-band rejection antennas cannot help but being large in size with many band rejection elements on the feed line of the antenna [9] and having a complex structure including via such as [18].

To circumvent the above shortcomings, the complementary split ring resonator (CSRR) was used as a band rejection element. The presented resonators in this study have co-directional gap of split rings. It is different to the conventional CSRR with reverse split rings. By etching the CSRR at an optimal position in the antenna, the aforementioned problems of mutual coupling and space restriction of the earlier multi-band rejection UWB antenna were solved. This main idea has made it possible to have excellent rejection performance at all rejection bands, controllability of each rejection band, and an easier fabrication of antenna with only a single-layer and a single sided metal shape which couldn't be achieved by the earlier quadruple-band rejection UWB antennas. Then, the fabrication and measurement of the finally proposed quadruple-band rejection UWB antenna were carried out in order to prove the validity of the design that was aforementioned.

2. ANTENNA DESIGN

2.1. Complementary Split Ring Resonator

The SRR structure is formed by two concentric metallic rings with a split on opposite sides, and the CSRR is the negative image of the SRR, as shown in Figures 1(a) and (b) [19]. SRR and CSRR are electrically small LC resonant elements with a high quality factor at microwave frequency and have been used as a periodic structure of metamaterial. So, the resonance characteristics of the CSRR have attracted the attention of the frequency-selective structure designer. In this paper, the CSRR is used as a band rejection element in the UWB antenna because CSRR structure is more suitable to be mounted on the planar structure than the SRR [20]. The narrow band resonance characteristics of the CSRR are affected in only the target frequency band and geometrical region on the UWB antenna. It is a key to solve the mutual coupling among the band rejection elements. Furthermore, the CSRR provides enough space on the conventional compact UWB antenna to embed the band rejection elements due to the sub-wavelength resonant structure of the CSRR.

Figure 1(c) is a conventional rectangular CSRR, which only has a difference of shape from Figure 1(b). But the basic principle of that is that it has the same mechanism as a typical CSRR. In this paper, the co-directional CSRR was used as shown in Figure 1(d). This CSRR behaves like the LC resonator from the same conventional CSRR shown in Figures 1(b) and (c), but the split ring gap differed from the conventional one. The orientation of the CSRR's ring gap and exciting field are interlinked. They affect the operation and resonance characteristics of the CSRR [21]. Therefore, the orientation of the ring gap is decided by the optimization work of the simulation in this paper. Use of the co-directional CSRR could simplify the process of the orientation decision of the ring gap and entire antenna design. It may be of interest to note that the study of band rejection UWB antenna was reported in [21] included the experimental demonstration for usefulness of the co-directional SRR, although it is one of various studies.

(a)   (b)   (c)   (d)
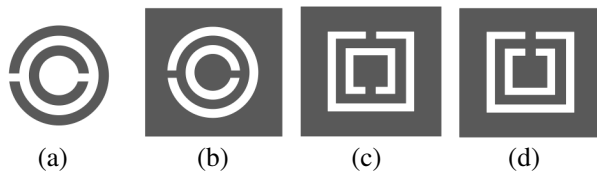
Figure 1. SRR and CSRR. (a) SRR. (b) CSRR. (c) Conventional CSRR. (d) Co-directional CSRR.
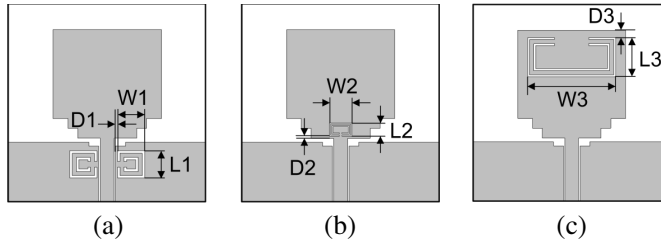
2.2. Basic Band Rejection UWB Antenna

Figure 2 shows the configuration and dimension of the proposed primitive UWB antenna design for the final structure. This antenna is constructed on Rogers4003 substrate with a thickness of 0.812 mm, a relative dielectric constant of 3.38, and a loss tangent of 0.0027. The coplanar waveguide (CPW) fed is applied to the antennas. It takes advantages of easy manufacturing and being cost efficient because the antenna and feed line are etched on the same plane using only one layer of substrate with a single-sided metallization. This paper compares the primitive UWB antenna without the CSRR (Figure 2) with the basic band rejection UWB antennas having only an individual CSRR (Figure 3), because when the results are compared it can aid in the design of the proposed antenna.
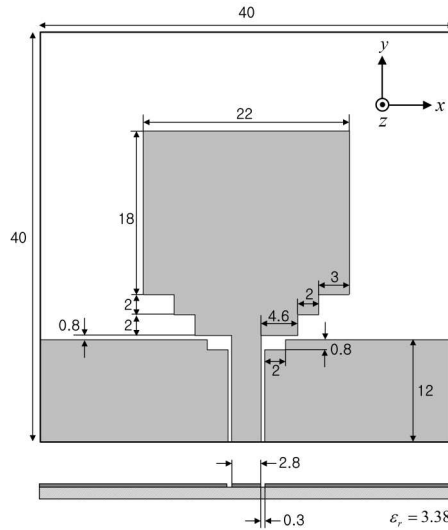
Figure 2. Geometry of the primitive UWB antenna.

Figure 3 shows the etched structure of the primitive UWB antenna including the individual CSRR. The Type 1 antenna with the WLAN/WiMAX 5 GHz band rejection function has been designed with the primitive UWB antenna by embedding the CSRRs in the antenna feeding location. The CSRRs were symmetrically disposed in a pair beside the CPW feed line to obtain the omni-directional radiation pattern at resonance frequency, and the split gaps of those were etched toward the feed line. To achieve the ITU 8 GHz band rejection performance, the Type 2 antenna employed a CSRR which

Figure 3. Basic band rejection UWB antenna including each CSRR. (a) Type 1. (b) Type 2. (c) Type 3.

has a split gap at the bottom part of the radiation patch. The Type 3 antenna has two independent rejection bands due to the inner ring and outer ring. The resonance frequency of the inner and outer ring corresponds entirely to the rejection bands of 2.4–2.6 GHz WLAN/WiMAX/S-DMB and 3.5 GHz WiMAX, respectively. Both orientations of the split gap of these rings are faced toward the y axis. Generally speaking, conventional CSRR exhibits a very narrow band due to the tight coupling between two rings. On the contrary, two rings employed in Type 3 antenna are in loosely coupled mode such that they exhibit two rejection bands.

The rejected frequency of each basic band rejection UWB antenna is forced to be the resonance frequency of the CSRR. The resonance frequency ω_0 of the CSRR can be expressed as (1) [5].

$$\omega_0 = \sqrt{\frac{2}{\pi r_0 LC}} \tag{1}$$

where L is the per unit length inductance between the ring slots, and C is the total capacitance of the CSRR. And r_0 is the average radius of the rectangular ring slots. As revealed in (1), resonance frequency ω_0 depends on its geometrical parameters.

Figure 4 represents the tuning effect by size and position of each CSRR on the basic band rejection UWB antenna. With adjustment of the size of each CSRR, the rejection bands of each antenna in Figure 3 can be tuned to the desired value. Figure 5 shows the influence of the gap angle of CSRRS on the VSWR. As mentioned earlier, the orientation of the CSRR should be considered when the CSRRs were positioned on the UWB antenna because the CSRR possessed inherent anisotropy depending on the direction of the exciting field. Thus, the band rejection performance is influenced by the position and the orientation of the CSRRs, which might lead to the discovery of the optimum value. Figure 6 shows the simulated VSWR curves of the primitive UWB antenna and three types of basic band rejection UWB

(a)

(b)

(c)
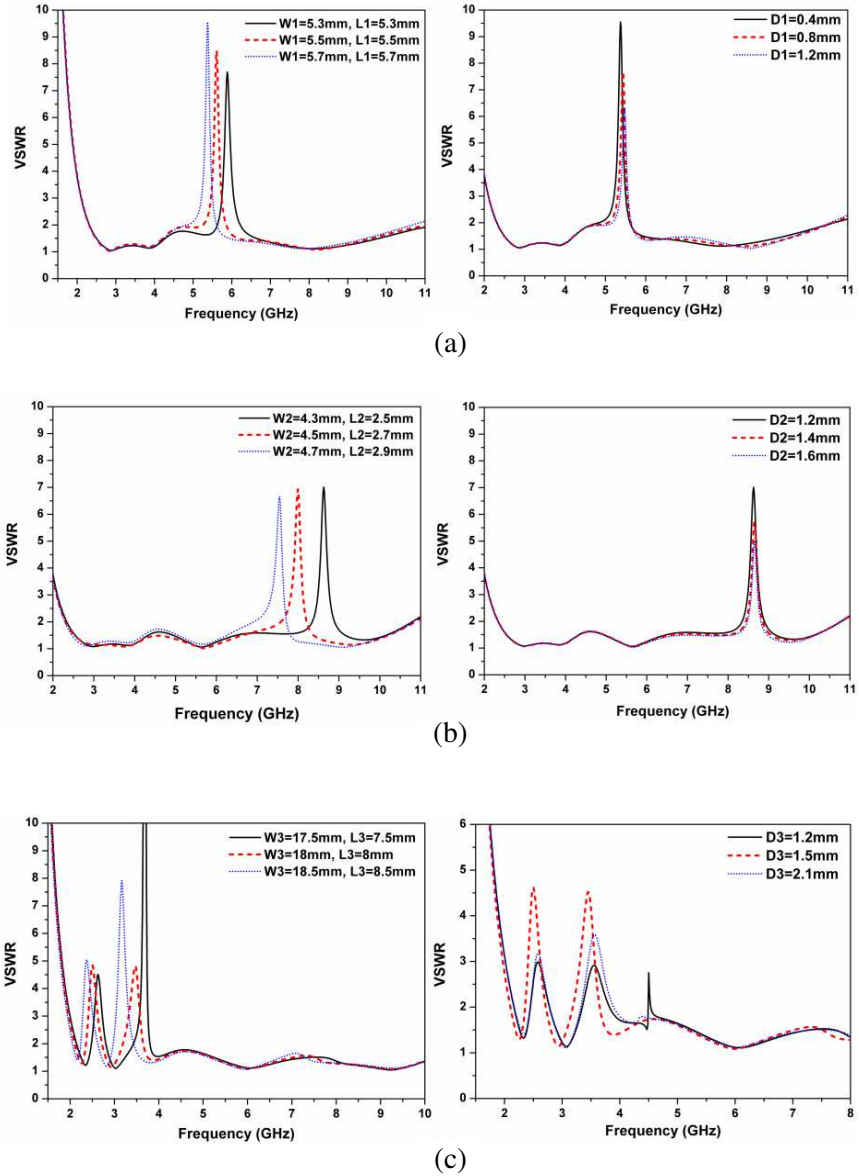
Figure 4. The simulated VSWR on the basic band rejection UWB antennas in terms of the size and position for each CSRR. (a) Type 1. (b) Type 2. (c) Type 3.
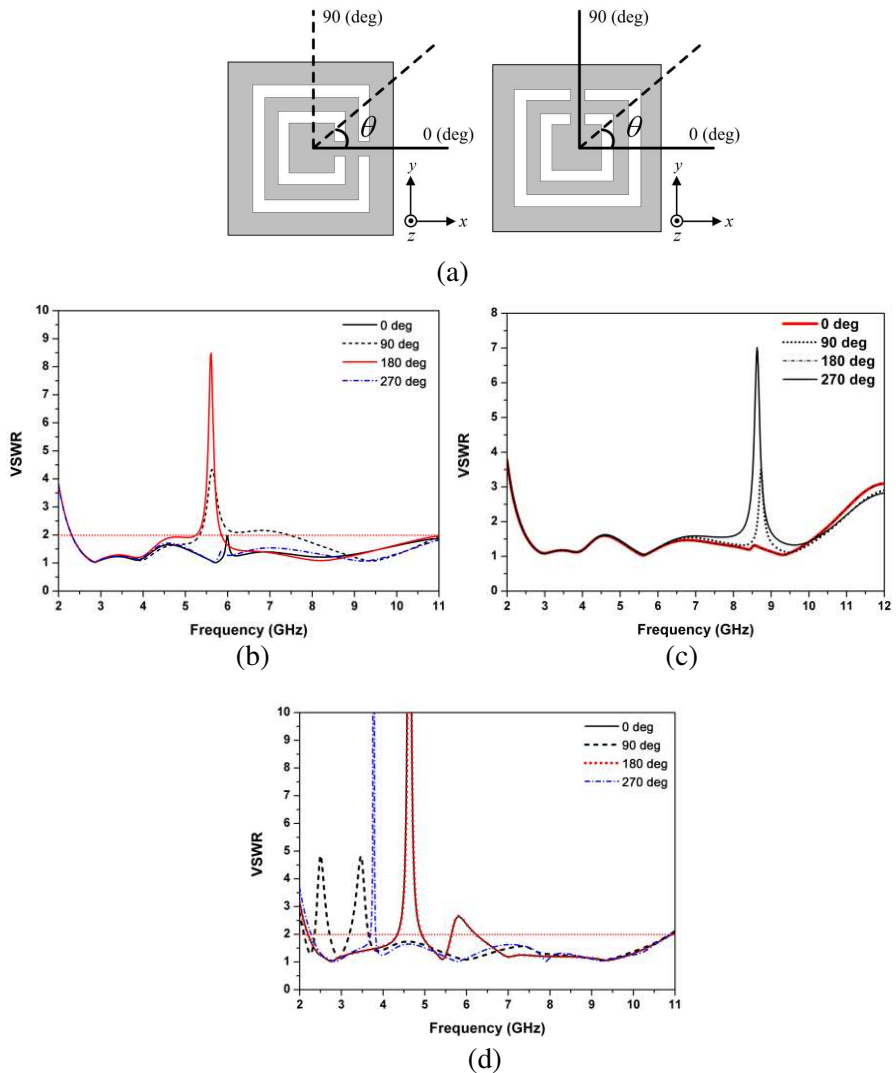
Figure 5. The simulated VSWR on the basic band rejection UWB antennas in terms of the orientation of the CSRRs. (a) Orientation angle of the CSRR. (b) Type 1. (c) Type 2. (d) Type 3.

antennas. This reveals that each type of antenna fulfills its own target rejection performance. From this result, the possibility of designing a quadruple band rejection UWB antenna by a spatial overlap of three types of individual antenna in Figure 3 can be possible.
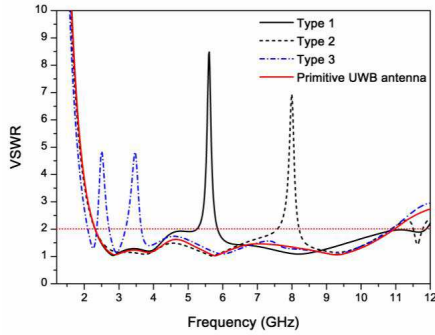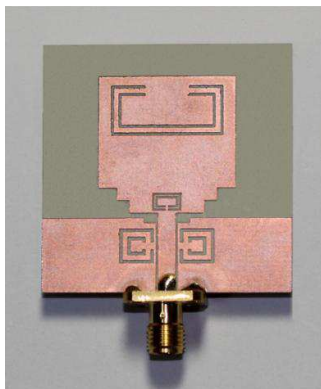
**Figure 6.** VSWR of the Type 1, Type 2, Type 3, and the primitive UWB antenna.
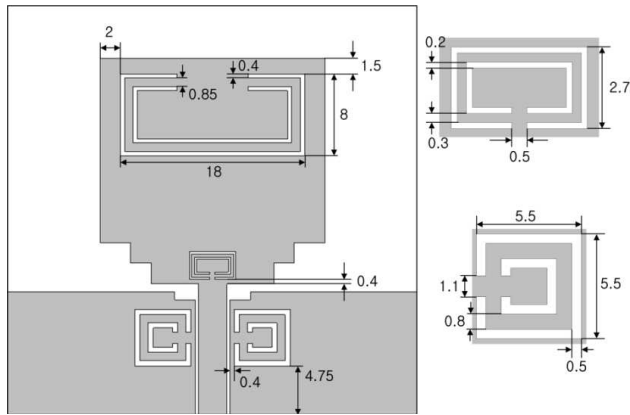
Figure 7. Geometry of the proposed quadruple-band rejection UWB antenna.

2.3. Quadruple-band Rejection UWB Antenna

Figure 7 shows the geometry of the finalized design antenna. The antenna consists of etching three kinds of CSRRs on the primitive UWB antenna as shown in Figure 2. The dimensions of the antenna are maintained as the previously determined primitive UWB antenna and holds for all three types of UWB antennas. Three CSRRs have its own inherent notch bands. Arrangement of the proposed CSRRs and orientation of the ring gap are optimized to achieve the performance of the targeted band rejection function. Figure 8 shows the photograph of the fabricated quadruple band rejection UWB antenna.

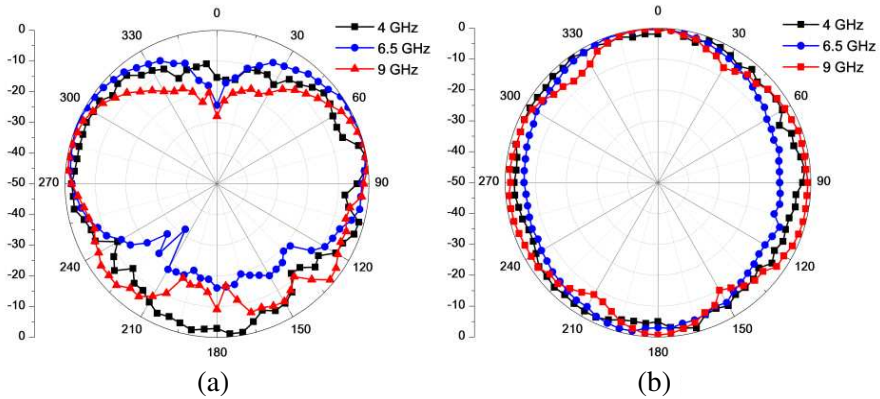**Figure 8.** Photograph of the proposed quadruple-band rejection UWB antenna.
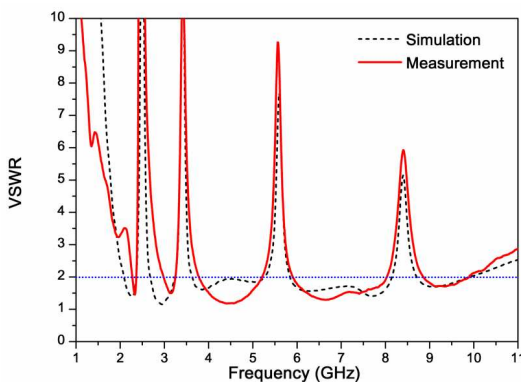
Figure 9. Simulated and measured VSWR of the proposed quadruple-band rejection UWB antenna.

3. SIMULATED AND MEASURED RESULTS

The simulated and measured VSWR of the finally proposed antenna are illustrated in Figure 9. This result clearly indicates that the proposed antenna covers the UWB band (VSWR ≤ 2) with quadruple sharp, rejected bands (VSWR > 2) of 2.37–2.9, 3.27–3.76, 5.2–5.89, and 8.06–8.8 GHz. The measurement and simulation were performed by an Anritsu 38397C network analyzer and the CST Microwave Studio, respectively. The rejection characteristics of each antenna type, as shown in Figure 6, are reflected in the result of Figure 9. In comparing and analyzing between Figure 6 and Figure 9, maintaining each rejection band after combination of individual antenna are observed. In other words, it means that mutual coupling between each type was minimized. If this mutual coupling was not negligibly small, the close similarity of the VSWR curve between them would have been disappeared.

The measured radiation patterns of the E-plane (yz-plane) and the H-plane (xz-plane) of the proposed antenna at the pass band (among the quadruple notch bands) frequencies of 4, 6.5, and 9 GHz are illustrated in Figure 10. The patterns have been measured in anechoic chamber at a distance of far field configuration. It can be observed that the patterns are approximately omnidirectional and similar to the pattern of the typical monopole antenna. In addition, the realized gain shown in Figure 11 displays the drop of antenna gain at the four places of intended rejection bands. This clearly indicates the effect of band

Figure 10. Measured radiation patterns of the proposed quadruple-band rejection UWB antenna at different UWB bands. (a) *E*-plane (*yz*-plane). (b) *H*-plane (*xz*-plane).
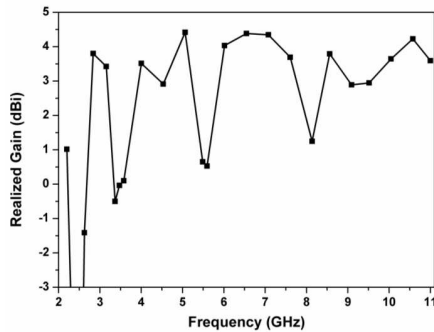

Figure 11. Realized gain of the proposed quadruple-band rejection UWB antenna.

rejection characteristics with CSRRs. Figure 12 shows the simulated surface current distributions at each rejection band. The applied power to the antenna is 1 Watt. The large current distribution is indicated in the dark color, and the small one is light. It is seen that the resonant surface currents are highly concentrated on each CSRR corresponding with rejection bands at operating frequency bands of each resonator. It means that a large portion of electromagnetic energy of the antenna at these bands has been stored in each CSRR as a non-radiating energy so that the radiation efficiency was dropped over the rejection bands, as seen in Figure 11. Once again, Figure 11 confirms the relevant four null
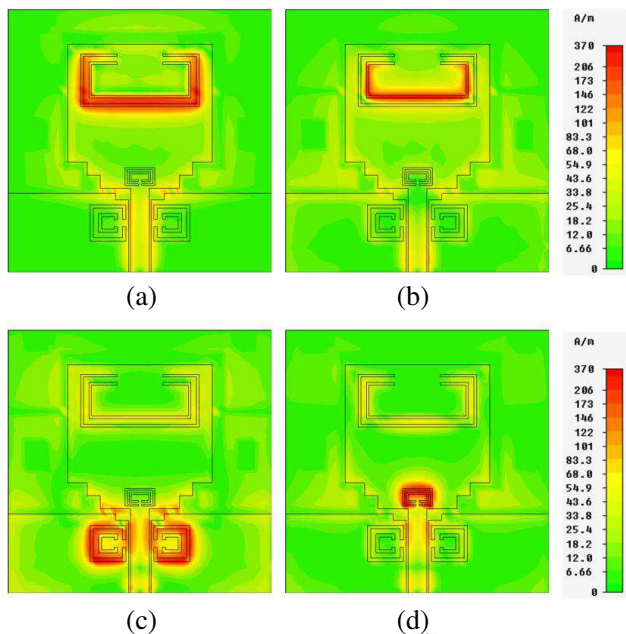
Figure 12. Surface current distribution of the proposed quadruple-band rejection UWB antenna at (a) 2.4 GHz, (b) 3.5 GHz, (c) 5.5 GHz, (d) 8.2 GHz.
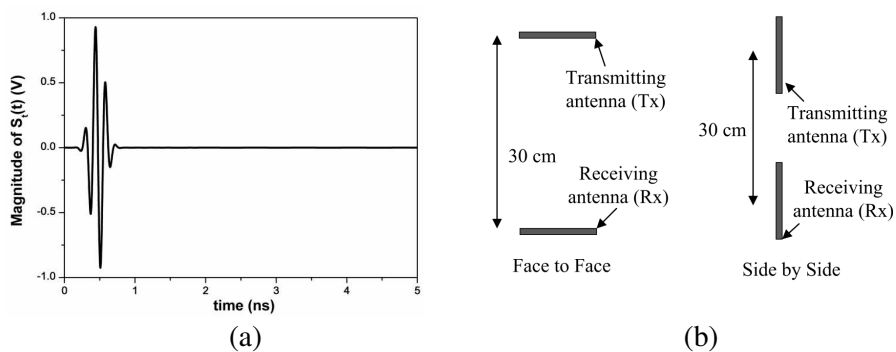
Figure 13. Input signal of the transmitting antenna and simulation setup. (a) Magnitude of input signal $s_t(t)$. (b) Fidelity factor simulation setup for each case.

positions over what we are in pursuit of the quadruple-band rejection performance.

To obtain the time domain response of the UWB antenna in

Table 1. Fidelity factor between transmitted and received signals.

	Tx: Primitive Rx: Primitive	Tx: Primitive Rx: Quadruple
Face to Face	0.92	0.93
Side by Side	0.85	0.79

Figure 7, it is assumed that the primitive UWB antenna as shown in Figure 2 is connected as the transmitting antenna, while the proposed antenna in Figure 7 plays the role of the receiving antenna. The two antennas are aligned pointing face-to-face and side by side with a distance of 300 mm. Figures 13(a) and (b) show the transmitted pulse $s_t(t)$ and the simulation setup, respectively. This pulse simulation is performed by a CST Design Studio simulator. To verify the similarity between the transmitted pulse $s_t(t)$ and the received pulse $s_r(t)$, the fidelity factor F as given in (2) is used [22].

$$F = \max_{\tau} \int\limits_{-\infty}^{\infty} s_r(t - \tau)s_t(t)dt \qquad (2)$$

By substituting the two normalized pulse signals in (2), we have calculated the fidelity factor F and given them in Table 1. On calculating, to bypass the distorted signal in a transmitting antenna, the proposed UWB antenna shown in Figure 7 was solely dedicated as the receiving antenna since one would doubt on the signal purity due to the existence of the band notch characteristic in the frequency domain if used as a transmitter [23]. This can be considered as a very good result compared with the other research that has been conducted in [22–25]. It is evident that the proposed UWB antenna exhibits a good time domain performance in the view of operating UWB communication systems. Here, the antenna having $F = 1$ indicates the ideal, without distortion in the transmission system of the pulse signal.

4. CONCLUSION

We have designed, fabricated, and measured the quadruple band rejection UWB antenna with the controllability over the rejection bands. By applying three co-directional CSRRs, the minimized mutual coupling among each band rejection element can be obtained what was the main objective of this study. The proposed antenna has the advantage of convenient implementation and mostly cost

efficient. This is because the etching of the antenna and feed line are realized on a single-layer of substrate and a single sided metal plane resulting in the easier fabrication and moderate prices. The suggested antenna itself is loaded with a quadruple bandstop-filter-like function to block the unwanted signal from an external wireless device and to maintain the performance of the UWB system in a hostile radio environment caused by the various radio interferences. Accordingly, the proposed quadruple band rejection UWB antenna might be useful for constructing the UWB communication system to mitigate the abundant electromagnetic interferences.

REFERENCES

1. Zha, F. T., S. X. Gong, G. Liu, H. Y. Yang, and S. G. Lin, "Compact slot antenna for 2.4 GHz/UWB with dual band-notched characteristic," *Microwave and Optical Technology Letters*, Vol. 51, No. 8, 1859–1862, 2009.

2. Li, Y. C. and K. J. Hung, "Compact ultrawideband rectangular aperture antenna and band-notched designs," *IEEE Transactions on Antennas and Propagation*, Vol. 54, No. 11, 3075–3081, 2006.

3. Xiao, J. X., M. F. Wang, and G. J. Li, "A novel UWB circinal slot antenna with band-notched characteristics," *Journal of Electromagnetic Waves and Applications*, Vol. 23, No. 10, 1377–1384, 2009.

4. Lee, W. S., D. Z. Kim, K. J. Kim, and J. W. Yu, "Wideband planar monopole antenna with dual band-notched characteristics," *IEEE Transaction on Microwave Theory and Techniques*, Vol. 54, No. 6, 2800–2806, 2006.

5. Kim, D. O., N. I. Jo, D. M. Choi, and C.-Y. Kim, "Design of the ultra-wideband antenna with 5.2 GHz/5.8 GHz band rejection using rectangular split-ring resonators (SRRs) loading," *Journal of Electromagnetic Waves and Applications*, Vol. 23, No. 17–18, 2503–2512, 2009.

6. Hu, Y. S., M. Li, G. P. Gao, J. S. Zhang, and M. K. Yang, "A double-printed trapezoidal patch dipole antenna for UWB applications with band-notched characteristic," *Progress In Electromagnetics Research*, Vol. 103, 259–269, 2010.

7. Su, M., Y. A. Liu, S. L. Li, and C. P. Yu, "A compact open slot antenna for UWB applications with band-notched characteristic," *Journal of Electromagnetic Waves and Applications*, Vol. 24, No. 14–15, 2001–2010, 2010.

8. Soltani, S., M. N. Azarmanesh, and P. Lotfi, "Design

of band notched CPW-FED monopole antenna using two symmetric parasitic elements for UWB applications," *Journal of Electromagnetic Waves and Applications*, Vol. 23, No. 11–12, 1407–1416, 2009.

9. Zhang, Y., W. Hong, C. Yu, Z. Q. Kuai, Y. D. Don, and J. Y. Zhou, "Planar ultrawideband antennas with multiple notched bands based on etched slots on the patch and/or split ring resonators on the feed line," *IEEE Transactions on Antennas and Propagation*, Vol. 56, No. 9, 3063–3068, 2008.

10. Yeo, J., "Wideband circular slot antenna with tri-band rejection characteristics at 2.45/5.45/8 GHz," *Microwave and Optical Technology Letters*, Vol. 50, No. 7, 1910–1914, 2008.

11. Wang, M. F., J. X. Xiao, and S. W. Wang, "Study of a dual-band notched wideband circular slot antenna," *Journal of Electromagnetic Waves and Applications*, Vol. 24, No. 17–18, 2445–2452, 2010.

12. Gong, J. G., Q. Li, G. Zhao, Y. Song, and Y. C. Jiao, "Design and analysis of a printed UWB antenna with multiple band-notched characteristics," *Journal of Electromagnetic Waves and Applications*, Vol. 23, No. 13, 1745–1754, 2009.

13. Yang, B., Y. C. Jiao, H. H. Xie, Z. Hong, and R. Zou, "A novel tri-band-notched ultra-wideband monopole antenna with coupled resonators," *Journal of Electromagnetic Waves and Applications*, Vol. 24, No. 14–15, 2019–2028, 2010.

14. Yang, Y. B., F. S. Zhang, L. Zhang, S. Gai, and J. G. Gong, "Design of a dual band-notched ultra-wideband antenna," *Journal of Electromagnetic Waves and Applications*, Vol. 23, No. 17–18, 2279–2287, 2009.

15. Ren, L. S., F. Li, J. J. Zhao, G. Zhao, and Y. C. Jiao, "A novel compact UWB antenna with dual band-notched characteristics," *Journal of Electromagnetic Waves and Applications*, Vol. 24, No. 11–12, 1521–1529, 2010.

16. Li, X., L. Yang, S. X. Gong, and Y. J. Yang, "Ultra-wideband monopole antenna with four-band-notched characteristics," *Progress In Electromagnetics Research Letters*, Vol. 6, 27–34, 2009.

17. Abbosh, A. M. and M. E. Bialkowski, "Design of UWB planar band-notched antenna using parasitic elements," *IEEE Transactions on Antennas and Propagation*, Vol. 57, No. 3, 796–799, 2009.

18. Dong, Y. D., W. Hong, Z. Q. Kuai, C. Yu, Y. Zhang, J. Y. Zhou, and J. X. Chen, "Development of ultrawideband antenna with

multiple band-notched characteristics using half mode substrate integrated waveguide cavity technology," *IEEE Transactions on Antennas and Propagation*, Vol. 56, No. 9, 2894–2902, 2008.

19. Falcone, F., T. Lopetegi, J. D. Baena, R. Marqués, F. Martín, and M. Sorolla, "Effectiv negative-ε stop-band microstrip lines based on complementary split ring resonators," *IEEE Microwave and Wireless Components Letters*, Vol. 14, No. 6, 280–282, 2004.

20. Baena, J. D., J. Bonache, F. Martin, R. Marqués, F. Falcone, T. Lopetegi, M. A. G. Laso, J. G. Garcia, I. Gil, M. F. Portillo, and M. Sorolla, "Equivalent-circuit models for split-ring resonators and complementary split-ring resonators coupled to planar transmission lines," *IEEE Transaction on Microwave Theory and Techniques*, Vol. 53, No. 4, 1451–1461, 2005.

21. Wang, W., S. Gong, Z. Cui, J. Liu, and J. Ling, "Dual band-notched ultra-wideband antenna with codirectional SRR," *Microwave and Optical Technology Letters*, Vol. 51, No. 4, 1032–1034, 2009.

22. Li, X., S. C. Hagness, M. K. Choi, and D. W. van der Weide, "Numerical and experimental investigation of an ultrawideband ridged pyramidal horn antenna with curved launching plane for pulse radiation," *IEEE Antennas and Wireless Propagation Letters* Vol. 56, No. 9, 3063–3068, 2008.

23. Akhoondzadeh-Asl, L., M. Fardis, A. Abolghasemi, and G. Dadashzadeh, "Frequency and time domain characteristic of a novel notch frequency UWB antenna," *Progress In Electromagnetics Research*, Vol. 80, 337–348, 2008.

24. Zheng, Z. A. and Q. X. Chu, "Compact CPW-fed UWB antenna with dual band-notched characteristics," *Progress In Electromagnetics Research Letters*, Vol. 11, 83–91, 2009.

25. Kanj, H., and M. Popović, "A novel ultra-compact broadband antenna for microwave breast tumor detection," *Progress In Electromagnetics Research*, Vol. 86, 169–198, 2008.